AMERICAN SOCIETY FOR MICROBIOLOGY | Antimicrobial Agents and Chemotherapy®

EXPERIMENTAL THERAPEUTICS

Linker Editing of Pneumococcal Lysin ClyJ Conveys Improved Bactericidal Activity

Hang Yang,[a,b] Dehua Luo,[c] Irina Etobayeva,[b,d] Xiaohong Li,[a] Yujing Gong,[c] Shujuan Wang,[a] Qiong Li,[e] Poshi Xu,[f,g] Wen Yin,[c] Jin He,[c] Daniel C. Nelson,[b,d] Hongping Wei[a]

[a]CAS Key Laboratory of Special Pathogens and Biosafety, Center for Emerging Infectious Diseases, Wuhan Institute of Virology, Chinese Academy of Sciences, Wuhan, China
[b]Institute for Bioscience and Biotechnology Research, University of Maryland, Rockville, Maryland, USA
[c]State Key Laboratory of Agricultural Microbiology, College of Life Science and Technology, Huazhong Agricultural University, Wuhan, China
[d]Department of Veterinary Medicine, University of Maryland, College Park, Maryland, USA
[e]Wuhan Polytechnic University, Wuhan, China
[f]Henan Provincial People's Hospital, Fuwai Central China Cardiovascular Hospital, Zhengzhou, Henan, China
[g]School of Clinical Medicine, Henan University, Zhengzhou, Henan, China

ABSTRACT *Streptococcus pneumoniae* is a leading human pathogen uniquely characterized by choline moieties on the bacterial surface. Our previous work reported a pneumococcus-specific chimeric lysin, ClyJ, which combines the CHAP (cysteine, histidine-dependent amidohydrolase/peptidase) enzymatically active domain (EAD) from the PlyC lysin and the cell wall binding domain (CBD) from the phage SPSL1 lysin, which imparts choline binding specificity. Here, we demonstrate that the lytic activity of ClyJ can be further improved by editing the linker sequence adjoining the EAD and CBD. Keeping the net charge of the linker constant, we constructed three ClyJ variants containing different lengths of linker sequence. Circular dichroism showed that linker editing has only minor effects on the folding of the EAD and CBD. However, thermodynamic examination combined with biochemical analysis demonstrated that one variant, ClyJ-3, with the shortest linker, displayed improved thermal stability and bactericidal activity, as well as reduced cytotoxicity. In a pneumococcal mouse infection model, ClyJ-3 showed significant protective efficacy compared to that of the ClyJ parental lysin or the Cpl-1 lysin, with 100% survival at a single ClyJ-3 intraperitoneal dose of 100 μg/mouse. Moreover, a ClyJ-3 dose of 2 μg/mouse had the same efficacy as a ClyJ dose of 40 μg/mouse, suggesting a 20-fold improvement *in vivo*. Taking these results together, the present study not only describes a promising pneumococcal lysin with improved potency, i.e., ClyJ-3, but also implies for the first time that the linker sequence plays an important role in determining the activity of a chimeric lysin, providing insight for future lysin engineering studies.

KEYWORDS bacteriophage lysin, chimeric lysin, *Streptococcus pneumoniae*, linker editing, antimicrobial therapy, bacteriophage, chimera, lysin

Streptococcus pneumoniae is a Gram-positive pathogen that causes a large range of infections, from superficial otitis media to severe invasive diseases, such as meningitis and community-acquired pneumonia (1, 2). Due to the increased transmission of antimicrobial resistance and the lack of efficient vaccines that can cover all pneumococcal serotypes (3), *S. pneumoniae* continues to be responsible for an annual 1.3 million deaths in children younger than 5 years old (4). A global retrospective investigation also revealed that drug-resistant *S. pneumoniae* is an alarming threat worldwide (5). This urgent situation prompted the U.S. Centers for Disease Control and Prevention

Citation Yang H, Luo D, Etobayeva I, Li X, Gong Y, Wang S, Li Q, Xu P, Yin W, He J, Nelson DC, Wei H. 2020. Linker editing of pneumococcal lysin ClyJ conveys improved bactericidal activity. Antimicrob Agents Chemother 64:e01610-19. https://doi.org/10.1128/AAC.01610-19.

Address correspondence to Hang Yang, yangh@wh.iov.cn, Daniel C. Nelson, nelsond@umd.edu, or Hongping Wei, hpwei@wh.iov.cn.

Received 8 August 2019
Returned for modification 21 October 2019
Accepted 18 November 2019
Accepted manuscript posted online 25 November 2019
Published 27 January 2020

(CDC) to call for aggressive and immediate action to halt the spread of drug-resistant pathogens (6). In this context, bacteriophage and bacteriophage-derived therapeutics are progressively attracting interest as alternative antimicrobials.

One group of promising bacteriophage-derived therapeutics are peptidoglycan hydrolases, known as endolysins, or lysins, which selectively digest select bonds of the peptidoglycan and lead to lysis of the host bacterium "from within" (7). Lysins alone are capable of directly killing Gram-positive bacteria with high efficacy when added exogenously as recombinant proteins, a process known as lysis "from without" (8, 9). Lysin-based experimental therapies have shown efficacy in several animal infection models (10–12), and some are currently being evaluated in human clinical trials, including the *Staphylococcus aureus*-targeted lysins CF-301 (ClinicalTrials.gov registration no. NCT03163446) and SAL-200 (ClinicalTrials.gov registration no. NCT03089697).

Lysins derived from bacteriophage that target Gram-positive bacteria usually consist of two distinct functional domains, an N-terminal enzymatically active domain (EAD) responsible for the murein hydrolase activity and a C-terminal cell wall binding domain (CBD) that usually recognizes specific secondary cell wall polysaccharides of a target bacterium (7). These two domains are intrinsically connected by a linker sequence, whose function has yet to be fully understood.

Choline moieties located in the pneumococcal teichoic and lipoteichoic acids serve as the binding substrate for several pneumococcal lysins, including Pal (13) and Cpl-1 (14), as well as the major autolysin of pneumococci, LytA (15). The CBDs of these enzymes contain homologous choline binding modules (CBMs) responsible for this binding specificity (16). One notable exception is the Cpl-7 lysozyme, encoded by the pneumococcal Cp-7 bacteriophage, whose CBD is made of three identical CW_7 repeats that share low homology to the CBMs and has been shown to bind directly to the peptidoglycan rather than the choline-containing teichoic acids (17). For the enzymes that do contain CBMs, binding to choline triggers dimerization of the enzymes, and this dimerization has been shown to be necessary for full peptidoglycan hydrolytic activity, at least in the case of the Cpl-1 lysozyme and the LytA amidase (18, 19).

Our previous work reported engineering of a pneumococcus-specific chimeric lysin, ClyJ, which contains a unique CHAP (cysteine, histidine-dependent amidohydrolase/peptidase) EAD and a typical CBM-containing CBD (20). In the present study, we further demonstrate that ClyJ forms a choline-dependent dimer and that its bactericidal activity can be improved by additional engineering of the linker sequence. Notably, one such engineered construct, ClyJ-3, was found to have improved activity *in vitro* and *in vivo* in a murine pneumococcal bacteremia model.

RESULTS

Design of ClyJ variants with linkers varying in length and flexibility. The chimeric lysin ClyJ is made up of a CHAP EAD that originated from the PlyC lysin and the CBD from gp20, a putative lysin encoded by the *Streptococcus* phage SPSL1 (20). The CBD of ClyJ contains a typical CBM that resembles CBMs from the pneumococcal autolysin LytA and the Cpl-1 lysin; i.e., it harbors six choline binding repeats and a C-terminal tail (see Fig. S1 in the supplemental material). Based on an understanding of the cooperative function between pneumococcal EADs and their CBDs, we hypothesized that the linker between EAD and CBD could play a role in facilitating the fitness of the EAD and CBD for their independent substrates located on the target bacterial cell wall. To test our hypothesis, we created several ClyJ variants *in silico* with linkers of various lengths. Previous studies have demonstrated that the charge of the EAD and/or CBD influences the activity of a lysin (21, 22). Therefore, to avoid introduction of such variables, we kept the net charge of the linker sequence constant in the design of the ClyJ variants (Fig. 1) by adding only neutrally charged glycine (G) or serine (S) amino acids (Fig. S2). The original linker of ClyJ is composed of the 24 amino acids (aa) preceding the CBD of gp20 as well as two nonnative GS amino acids introduced by BamHI during cloning. The ClyJ-1 and ClyJ-2 variants were designed with elongated

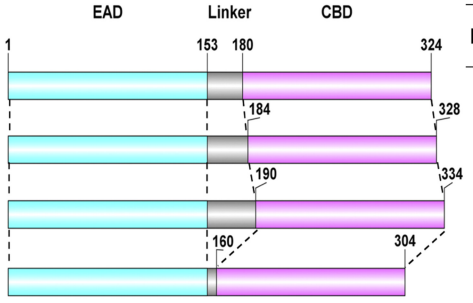

Protein	Flexibility (F)			
	F_{EAD}	$^*F_{Linker}$	F_{CBD}	F_{Total}
ClyJ	82.76	0.61	75.25	173.91
ClyJ-1	82.95	0.62	74.64	176.26
ClyJ-2	81.74	0.63	75.09	179.41
ClyJ-3	81.13	0.73	76.55	162.05

FIG 1 Schematic composition and characteristics of ClyJ and its variants. The CHAP EAD is labeled in cyan, the linker is in gray, and the CBM CBD is in purple. The start and end positions of each domain are indicated. The flexibility analysis was performed by using FlexPred online software (https://bio.tools/FlexPred). F_{EAD}, the flexibility of the enzymatically active domain; $^*F_{Linker}$, the flexibility of the linker divided by the number of amino acids in the linker; F_{CBD}, the flexibility of the cell wall binding domain; F_{Total}, the flexibility of the full-length lysin.

linkers, whereas ClyJ-3 had a significantly truncated linker (Fig. S2). Predicted flexibility analysis revealed that the linkers from the ClyJ variants showed a range in degrees of elasticity that influenced the overall flexibility of the EADs and CBDs (Fig. 1). Each ClyJ variant was then cloned, expressed in *Escherichia coli*, and purified as a soluble protein similar to the parental ClyJ (Fig. S3).

Linker editing shows minor influence on the structure of ClyJ variants. Because linker sequences have been shown to play a role in the structure-activity relationships of proteins (23, 24), we analyzed the secondary structure of ClyJ and its variants by circular dichroism (CD) to assess proper protein folding. Results showed that the spectra of ClyJ and ClyJ-1 most resemble each other (Fig. 2a and b) and that the spectra of ClyJ-2 and ClyJ-3 were also very similar to each other (Fig. 2c and d). However, the differences between the two groups are due to differences in the molar ellipticity

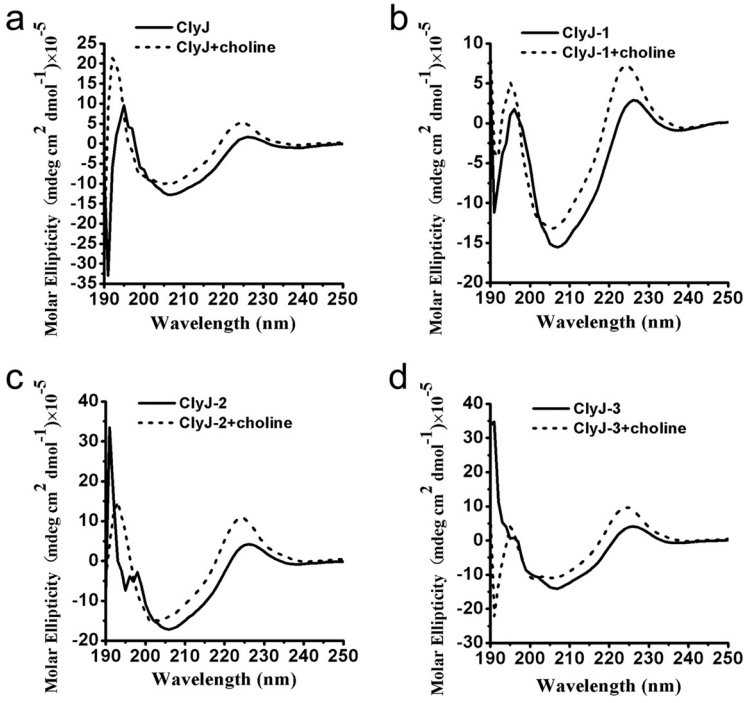

FIG 2 Circular dichroism spectra of ClyJ and its variants. The UV spectra of ClyJ (a), ClyJ-1(b), ClyJ-2 (c), and ClyJ-3 (d) were scanned from 190 to 260 nm (0.1-cm path length) at room temperature in the absence or presence of 50 mM choline.

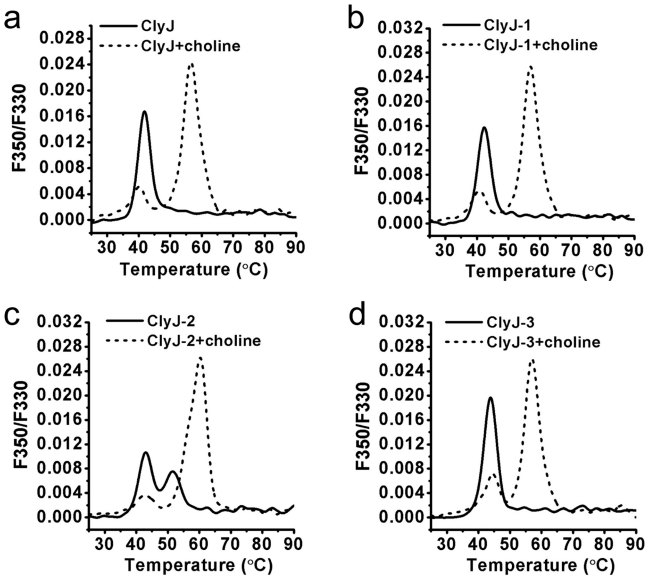

FIG 3 Thermal unfolding profiles for ClyJ and its variants. The profiles of ClyJ (a), ClyJ-1(b), ClyJ-2 (c), and ClyJ-3 (d) were determined by nanoDSF from 25 to 90°C in the absence or presence of 50 mM choline. Values on the *y* axis represent the first derivative of the ratio of fluorescence at 350 nm and 330 nm.

intensities. Minor changes in CD profiles were observed for the four proteins below 195 nm, which may due to the existence of an α-helix in the linker-editing region or optically active buffer components. However, all four proteins had UV peaks at 226 and 224 nm in the absence and presence of choline, respectively, suggesting similar folding and responses to choline in all four. Additional analysis revealed that the composition of the secondary structural components for all four enzymes is nearly identical (Table S1), and minor variations upon binding choline are uniformly seen in all variants. We further used I-TASSER to perform structural predictions for ClyJ and its variants. Each prediction showed a similar structure with a barrel-like EAD and a single layer β-hairpin contained within the CBD (Fig. S4). However, the predicted surface shape of ClyJ-3 is quite different from that of the other variants, showing a C-like shape, while the others displayed a straight-line shape (Fig. S4).

ClyJ-3 has improved thermal stability and forms a choline-dependent dimer. Next, we assessed the thermal stability of ClyJ and its variants using nano-differential scanning fluorimetry (nanoDSF). Results showed that the thermal transition temperature increases from 41.8°C for ClyJ to 43.8°C for ClyJ-3, the variant with the shortest linker sequence (Fig. 3a and d and Table S2). The single peaks noted for ClyJ, ClyJ-1, and ClyJ-3 indicate that the two domains, EAD and CBD, unfold together (Fig. 3a, b, and d). In contrast, ClyJ-2, with the longest linker, showed two transition temperatures, 43.1°C and 53.5°C, suggesting that the two functional domains unfold independently (Fig. 3c). In the presence of choline, two thermal transition peaks were noted for each enzyme, one near the transition temperature without choline and one ~15°C higher (Table S2). Presumably, the lower temperature represents the unfolding of the EAD, and the higher temperature is the transition of the CBD, stabilized by choline. Toward this end, the $BS(PEG)_9$ chemical cross-linker, a homobifunctional regent for covalent conjugation between amine-containing molecules, was used to confirm the presence of a dimer for ClyJ when it is exposed to 50 mM choline (Fig. S5), suggesting that the ClyJ variants should, like Cpl-1 and LytA, form choline-dependent dimers.

ClyJ-3 has improved lytic activity compared to that of ClyJ and Cpl-1. We evaluated the bactericidal activities of ClyJ and its variants against two pneumococcal strains, NS26 and NS20, under equal molar concentrations. The variants ClyJ-1 and ClyJ-2 maintained bactericidal activity comparable to that of the parental ClyJ, effecting a 3- to 4-log10 drop in viability in 60 min, depending on the strain (Fig. 4a and b). In

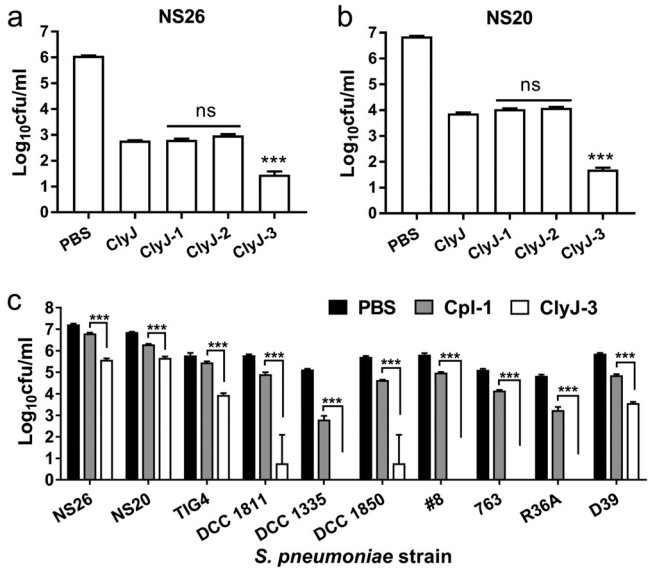

FIG 4 ClyJ-3 shows improved bactericidal activity. (a and b) Comparison of the bactericidal activities of ClyJ and its variants. *S. pneumoniae* NS26 or NS20 cells were treated with an equal molar concentration (0.69 μM) of either ClyJ or a variant at 37°C for 60 min, as indicated. (c) Comparison of the bactericidal activities of ClyJ-3 and Cpl-1. Multiple pneumococcal cells were treated with an equal molar concentration (0.29 μM) of ClyJ-3 or Cpl-1 at 37°C for 10 min. The number of residual CFU in each treatment was determined by plating 10-fold serial dilutions on THY agar and compared to that of the PBS-treated control by a two-tailed Student's *t* test. Data are shown as means ± standard deviations. ns, not significant; ***, $P < 0.001$.

contrast, ClyJ-3 exhibited significantly ($P < 0.001$) elevated bactericidal activity, effecting a ~1.32- and ~2.18-log10 increase in killing activity for *S. pneumoniae* NS26 and NS20, respectively, compared to activity of the parental ClyJ (Fig. 4a and b).

Next, we compared the bacteriolytic activities of ClyJ-3 and ClyJ against an extended range of streptococcal species, including an additional 18 *S. pneumoniae* strains, as well as representative strains of *Streptococcus mutans*, *Streptococcus gordonii*, *Streptococcus ratti*, *Streptococcus salivarius*, *Streptococcus parasanguinis*, and *Streptococcus intermedius* in a turbidity reduction assay. As shown in Fig. 5, all *S. pneumoniae* strains were as sensitive to ClyJ-3 as they were to ClyJ, and more than half (11/18) showed increased bacteriolytic sensitivity to ClyJ-3, including TIGR4, GB2092 (serotype 4), DCC1494 (serotype 14), 765, and DCC1335 (serotype 9 V). As expected, both ClyJ and ClyJ-3 were bacteriolytic only toward *S. pneumoniae* strains, highlighting the species-specific targeted nature of these enzymes.

We also benchmarked the bactericidal activity of ClyJ-3 to the well-known pneumococcal lysin, Cpl-1, against multiple pneumococcal strains using equal molar concentrations (0.29 μM) in a log-fold killing assay. The results showed that ClyJ-3 has a significantly higher ($P < 0.001$) bactericidal profile than Cpl-1 against all strains tested, with four of the strains (4/10) completely sterilized (Fig. 4c).

ClyJ-3 shows reduced cytotoxicity compared to that of ClyJ. Our previous study demonstrated cytotoxicity for ClyJ at concentrations of >250 μg/ml (20), a defect that may potentially halt its further pharmaceutical development. As a response to this issue, we ascertained the toxicity of ClyJ and ClyJ-3 to two different epithelial cell lines, Caco-2 and CHO-K1. Similar to what was previously observed, ClyJ showed notable toxicity against both cell lines at high doses, specifically, at >500 μg/ml for the Caco-2 cell line (Fig. 6a) and at >125 μg/ml for the CHO-K1 cell line (Fig. 6b). In contrast, >92% relative viability was observed for both cell lines after exposure to 500 μg/ml of ClyJ-3 (Fig. 6), indicating that ClyJ-3 has an improved safety profile compared to that of the ClyJ parental lysin.

ClyJ-3 shows improved protective efficacy in a mouse infection model. The above results suggest that ClyJ-3, with the shortest linker and least flexibility, has

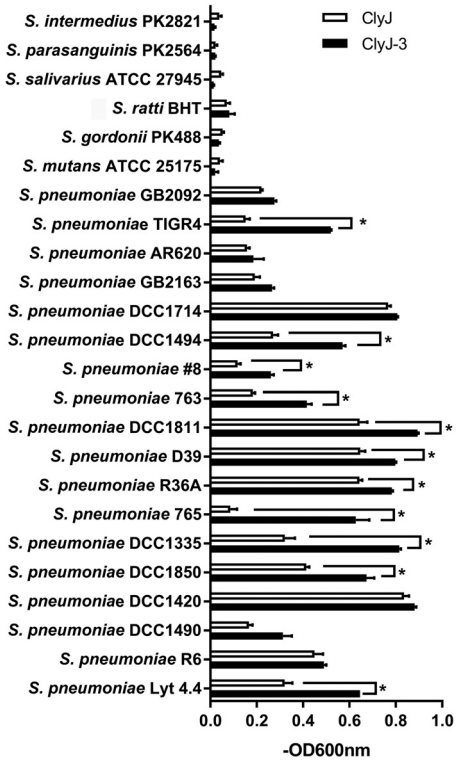

FIG 5 Expanded host range susceptibility. The susceptibility levels of various streptococcal strains to bacteriolytic activity of ClyJ or ClyJ-3 were tested in a turbidity assay. Each strain was treated with 25 μg/ml of ClyJ or ClyJ-3 for 20 min, and the decrease in the OD_{600} was recorded by a microplate reader. The activity of each lysin is expressed as the difference in the decrease in the OD_{600} between lysin-treated wells and PBS-treated wells [$-OD_{600}$ = (initial $OD_{600\ (\text{lysin-treated well})}$ − final $OD_{600\ (\text{lysin-treated well})}$) − (initial $OD_{600\ (\text{PBS-treated well})}$ − final $OD_{600\ (\text{PBS-treated well})}$)]. The lytic activity of ClyJ-3 was compared to that of ClyJ by a two-tailed Student's *t* test. Data are shown as means ± standard deviations. *, $P < 0.05$.

improved lytic and bactericidal activity over its parental lysin, ClyJ, as well as over the most studied natural pneumococcal lysin, Cpl-1. To further establish these findings *in vivo*, we assessed the protective efficacy of ClyJ-3 in a mouse pneumococcal septicemia model using a previously demonstrated pathogenic strain, *S. pneumoniae* NS26 (20). One hour after intraperitoneal administration of 8×10^7 CFU/mouse of NS26, mice were randomly separated into 8 therapeutic groups. As shown in Fig. 7a, ClyJ-3 fully protected mice (12/12) from lethal pneumococcal infection at a dose of 100 μg/mouse, and a dose of 50 μg/mouse provided 83% protection (10/12). ClyJ was less effective, providing 58% (7/12) and 50% (6/12) protection at doses of 100 and 50 μg/mouse, respectively. When the same experimental parameters were extended to Cpl-1, efficacy

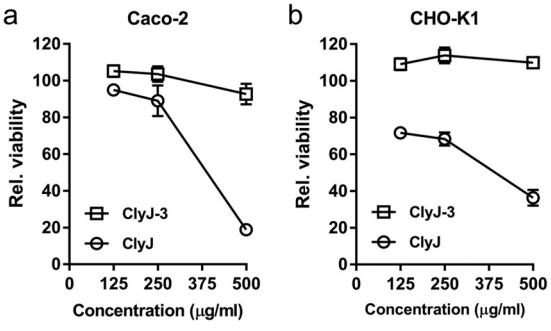

FIG 6 ClyJ-3 has reduced cytotoxicity compared to that of ClyJ. Caco-2 (a) and CHO-K1 (b) cells were exposed to different concentrations of enzyme (0, 125, 250, and 500 μg/ml) for 48 h, and the relative viability of cells after each treatment was determined by MTT assay.

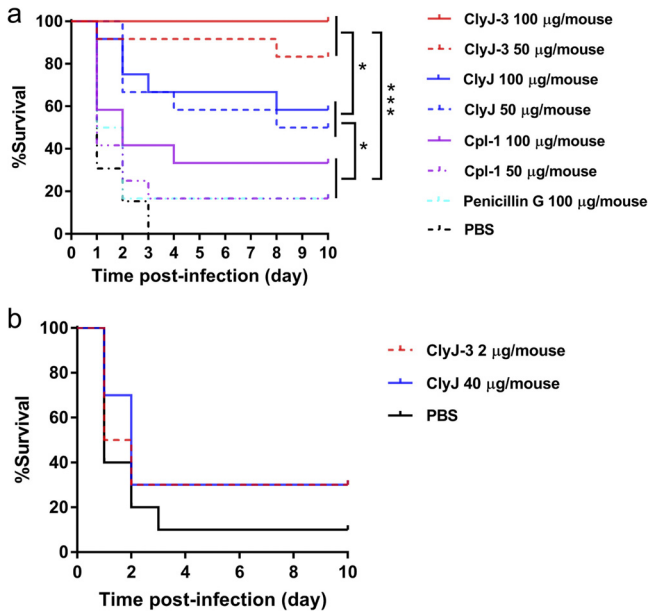

FIG 7 ClyJ-3 shows improved protective efficacy *in vivo*. (a) ClyJ-3 protects mice from lethal *S. pneumoniae* infection with higher efficacy than ClyJ and Cpl-1. Female BALB/c mice (6 to 8 weeks old) were injected intraperitoneally with 8×10^7 CFU/mouse of *S. pneumoniae* NS26 and divided randomly into 8 groups. At 1 h postinfection, groups ($n = 12$) received a single intraperitoneal dose of 50 or 100 μg/mouse of ClyJ, ClyJ-3, or Cpl-1, 100 μg/mouse of penicillin G, or an equal volume of PBS buffer. (b) Establishment of an equivalent dose of ClyJ and ClyJ-3 *in vivo*. Female BALB/c mice (6 to 8 weeks old) were injected intraperitoneally with 3.8×10^7 CFU/mouse of *S. pneumoniae* NS26. At 1 h postinfection, groups ($n = 12$) received a single intraperitoneal dose of 40 μg/mouse of ClyJ, 2 μg/mouse of ClyJ-3, or an equal volume of PBS buffer. The survival rates for all groups were recoded for 10 days. Survival curves were analyzed by log rank (Mantel-Cox) and Gehan-Breslow-Wilcoxon tests. *, $P < 0.05$; ***, $P < 0.01$.

fell to 30% (4/12) at 100 μg/mouse and to 17% (2/12) at 50 μg/mouse, the same efficacy as seen with penicillin G at 100 μg/mouse. Collectively, these results show that ClyJ-3 has significantly improved protective efficacy *in vitro* and *in vivo* compared to that of its parental lysin, ClyJ, and the natural lysin, Cpl-1.

We further compared the protective efficacies of ClyJ-3 and its parental lysin, ClyJ, in the pneumococcal mouse model with lower enzyme doses. As shown in Fig. 7b, an intraperitoneal injection of 3.8×10^7 CFU/mouse of *S. pneumoniae* NS26 caused a mortality rate of 90% (9/10) in the phosphate-buffered saline (PBS)-treated group, whereas 40 μg/mouse of ClyJ or 2 μg/mouse of ClyJ-3 protected 30% of infected mice (3/10). These results indicate that an equivalent dose of ClyJ-3 is about 20 times lower than that of its ClyJ parental lysin.

DISCUSSION

The increased emergence of antimicrobial-resistant *S. pneumoniae* is requiring global efforts to discover new therapeutics that have alternative mechanisms of action. Currently, bacteriophage-derived lysins are considered one of the most promising nontraditional therapeutics due to several unique attributes, including the following: (i) high efficacy/lytic activity, (ii) low possibility of evoking resistance, (iii) strict specificity for target pathogens, (iv) broad bacteriophage sources to derive new lysins, and (v) good feasibility for engineering. In this study, we reported a novel engineering strategy, i.e., linker optimization, for improving the lytic activity of a chimeric lysin, ClyJ, whose safety and efficacy profiles were demonstrated in our previous work (20).

Recent engineering efforts suggest that the EAD and CBD elements from different lysins can be fused to create novel combinations, or chimeric lysins, that are endowed with unique attributes. These include enhanced activity (25, 26), extended host range (27), reduced immunogenicity (28, 29), or elongated half-life (30, 31). While some of these studies were based on trial-and-error domain shuffling, others incorporated

rational bioengineering concepts. Out of this work, a few basic rules emerged that guide current engineering approaches, such as the charge of the functional domains. Because bacterial surface carbohydrates are usually negatively charged, lytic activities of lysins have been improved by enhancing the positive charge of the EAD (22) or by converting a negatively charged CBD to a positive charge (21). However, to date, the nature or length of the linker sequence between the EAD and CBD has not been taken into consideration for engineering efforts.

In the present study, we have demonstrated, for the first time, that the linker between the EAD and CBD also plays an important role in determining the activity of a lysin. The linker can influence the flexibility of the various domains through structure-function relationships. In the case of ClyJ-3, our analysis revealed that the predicted flexibility of the full-length protein was decreased despite the fact that the CBD increased in flexibility compared to levels in CBDs from other ClyJ variants. These traits were found to correlate to improved thermal stability and activity in ClyJ-3 compared to levels in parental ClyJ. Although it is not presently clear why modifications of the linker sequence affect the overall properties of the chimeric endolysin, several possibilities exist. Among these, the reduced overall flexibility of ClyJ-3 may increase its structural rigidity. Alternatively, the motion of the CBD relative to that of the EAD may be higher in ClyJ-3 than in the parental ClyJ.

Notwithstanding the above contributions of flexibility, it is also possible that the physical length of the linker could have an influence on the spatial distance between the EAD catalytic center and the CBD substrate binding center. To achieve efficient cell lysis, the EAD and the CBD should bind to their separate substrates simultaneously. If the linker is too short or too long, it would presumably disturb the cooperative mechanism of action of these two domains. Previous studies have demonstrated that the distance between the EAD catalytic center and choline binding site 2 is ~37 Å for Cpl-1 (32), indicating a defined distance between these two domains. Considering that the linker of ClyJ-3 (6 aa) is significantly shorter than that of its parental lysin ClyJ (26 aa), it is conceivable that the spatial distance between the EAD catalytic center and the choline binding center would change as a response to the varied linker length. On the other hand, the putative bent shape of ClyJ-3 reveals a shortened distance between the EAD catalytic center and the CBD binding center, which may be another factor contributing to the improved bactericidal properties. Although the predicated structures of ClyJ variants offer a clue to understand this statement, the crystal structures of ClyJ and its variants still need to be established.

In summary, we report here a novel strategy, i.e., linker optimization, to edit the chimeric lysin, ClyJ, for improved bactericidal activity. As a result, ClyJ-3 has been demonstrated to possess enhanced thermal stability, reduced cytotoxicity, and improved activity both *in vitro* and in an animal infection model. The editing strategy reported here not only creates potential candidates against pneumococcal infections but also provides new insights into understanding the rules for engineering chimeric lysins against other pathogens.

MATERIALS AND METHODS

Bacterial strains. Bacterial strains used in this study are listed in Table S3 in the supplemental material. *S. pneumoniae* strains were cultured in THY (Todd-Hewitt broth containing 0.5% yeast extract) medium statically at 37°C with 5% CO_2. Other Gram-positive bacteria were grown in brain heart infusion (BHI) broth at 37°C. *Escherichia coli* BL21(DE3) was grown in lysogeny broth (LB) medium.

Construction of ClyJ variants. ClyJ variants ClyJ-1, ClyJ-2, and ClyJ-3 were constructed by overlap PCR using site-specific primers (Table S4) according to standard methods described elsewhere (33). Specifically, for ClyJ-1 construction, primers ClyJ-1-F1, ClyJ-1-R1, ClyJ-1-F2, and ClyJ-1-R2 were used; for ClyJ-2, primers ClyJ-2-F1, ClyJ-2-R1, ClyJ-1-F2, and ClyJ-1-R2 were used; for ClyJ-3, primers ClyJ-1-F1, ClyJ-3-R1, ClyJ-3-F2, and ClyJ-1-R2 were used. All constructs were inserted in the NcoI and XhoI sites of a pET28b(+) vector, transformed into *E. coli* BL21(DE3) cells, and verified by direct DNA sequencing analysis.

Protein expression and purification. All proteins used in this study were purified from *E. coli* BL21(DE3) cells by nickel-nitrilotriacetic acid columns according to the supplier's instructions. Briefly, mid-log-phase cells were induced with 0.2 mM isopropyl β-D-thiogalactoside (IPTG), incubated at 16°C for 18 h, and harvested for protein purification. Column washing and eluting were performed with 60 and

250 mM imidazole, respectively. After being dialyzed against PBS buffer (137 mM NaCl, 2.7 mM KCl, 4.3 mM $Na_2HPO_4{\cdot}H_2O$, 1.4 mM KH_2PO_4, pH 7.4), collected proteins were then passed through a Detoxi-Gel endotoxin removing gel (Thermo Scientific), filter sterilized, and stored at 4°C until needed. The residual endotoxin level was determined by an EndoLISA kit (enzyme-linked immunosorbent assay [ELISA]-based endotoxin detection assay; Hyglos GmbH) according to the manufacturer's instructions and confirmed a low level of endotoxin (<0.5 endotoxin units [EU]/ml). Protein concentration was quantified by a Bradford assay, using bovine serum albumin (BSA) as a standard.

Bacteriolytic and bactericidal assays. Lysin bacteriolytic activity was measured via a turbidity reduction assay as described previously (34). Briefly, overnight cultures of bacteria were washed once with PBS (pH 7.4) and resuspended in PBS to a final optical density at 600 nm (OD_{600}) of ~1.0, and 190 μl of cells was incubated with 10 μl of each lysin (to a final concentration of 25 μg/ml) in 96-well plates (Corning, USA) at a total volume of 200 μl. The decrease of absorbance at OD_{600} was monitored every 15 s for 20 min on a SpectraMax 190 spectrophotometer (Molecular Devices, San Jose, CA). Controls were run in parallel and used an equal volume of PBS buffer in place of the enzyme. The activity of each lysin was expressed as the difference in the decrease of the OD_{600} at 20 min between lysin-treated wells and PBS-treated wells [$-OD_{600}$ = (initial $OD_{600\ (\text{lysin-treated well})}$ − final $OD_{600\ (\text{lysin-treated well})}$) − (initial $OD_{600\ (\text{PBS-treated well})}$ − final $OD_{600\ (\text{PBS-treated well})}$)].

The decrease in *S. pneumoniae* in viable cell number (i.e., bactericidal assay) after treatment with each lysin was determined by plating serial dilutions on THY agar. Specifically, for comparison of the lytic activities of ClyJ, ClyJ-1, ClyJ-2, and ClyJ-3, pneumococcal cells were treated with an equal final molar concentration of each lysin (0 or 0.69 μM [i.e., 23.5 μg/ml for ClyJ-3]) at 37°C for 60 min; for comparison of the activities between ClyJ-3 and Cpl-1, pneumococcal cells were treated with an equal final molar concentration of each lysin (0 or 0.29 μM [i.e., 10 μg/ml for ClyJ-3]) at 37°C for 10 min. Counts of residual CFU in each treatment were determined by plating 10-fold serial dilutions on THY agar and incubation overnight at 37°C. All experiments included at least three biological replicates.

Nano-differential scanning fluorimetry. The thermal stabilities of ClyJ and its variants were analyzed by a nano-differential scanning fluorimetry (nanoDSF) method using a Prometheus NT.48 instrument (NanoTemper Technologies, CA). The intrinsic emission fluorescence levels of each protein (100 μg/ml) at 350 and 330 nm were monitored over a temperature range of 25 to 90°C (increasing step of 0.8°C/min) in the absence or presence of 50 mM choline, using dialysis buffer without or with 50 mM choline as controls, respectively. The first derivative of the ratio of fluorescence at 350 nm and 330 nm (1st derivative of F_{350}/F_{330}) was calculated automatically by the PR.ThermControl software supplied with the instrumentation. Samples were measured in triplicates. The thermal unfolding transition temperature (T_m) corresponds to peaks of the 1st derivative of F_{350}/F_{330}.

Circular dichroism. The circular dichroism spectra of ClyJ (650 μg/ml), ClyJ-1 (1,000 μg/ml), ClyJ-2 (1,000 μg/ml), and ClyJ-3 (750 μg/ml) in 20 mM Tris-HCl (pH 8.0) were collected with an Applied Photophysics Chirascan Plus circular dichroism spectrometer (Leatherhead, UK) from 190 to 260 nm (0.1-cm path length) at room temperature in the absence or presence of 50 mM choline. The spectra of air and buffer were recorded as background and baseline, respectively. The secondary structure was calculated by the CDNN software, version 2.1, supplied by the instrument manufacturer.

Cross-linking analysis. To analyze polymerization, ClyJ was cross-linked with 1.5 mM $BS(PEG)_9$ (Sigma-Aldrich, Shanghai, China) in the absence or presence of 50 mM choline and run on a 12% SDS-PAGE gel.

Cytotoxicity determination. Caco-2 and CHO-K1 cells (~5×10^3 cells/well) were inoculated in a 96-well plate 1 day before the experiment. Cells were exposed to various concentrations of ClyJ or ClyJ-3 (0, 125, 250, and 500 μg/ml) for 24 h, and residual cell viability was determined by addition of 250 μg/ml MTT [3-(4,5-dimethylthiazol-2-yl)-2,5-diphenyltetrazolium bromide] and incubated for another 4 h. The resulting formazan salt in each well was dissolved with 200 μl of dimethyl sulfoxide (DMSO) and colorimetrically analyzed by a Synergy H1 microplate reader (BioTek, VT) at 570 nm. The relative viability of cells after each treatment was normalized and compared to that of the PBS-treated control wells.

Structure prediction of ClyJ and its variants. The three-dimensional (3D) structures of ClyJ and its variants were predicated by the I-TASSER online service (35) and further analyzed by PyMOL.

Mouse infection model. All mouse infection experiments were performed in an animal biosafety level 2 (ABSL-2) lab, and all experimental methods were carried out in accordance with the regulations and guidelines set forth by the Animal Experiments Committee of the Wuhan Institute of Virology, Chinese Academy of Sciences. All experimental protocols were approved by the Animal Experiments Committee of the Wuhan Institute of Virology, Chinese Academy of Sciences (WIVA17201602). During the experiment, animals were randomized and cared for in individually ventilated cages according to a set of animal welfare and ethical criteria, and euthanized at the end of observation.

In the mouse systemic infection model, female BALB/c mice (6 to 8 weeks old) were injected intraperitoneally with *S. pneumoniae* NS26 at a single dose of 8×10^7 CFU/mouse and divided randomly into multiple groups. Bacterial burdens in blood and organs at 1 h postinfection were confirmed by plating on THY agar as described previously (20). At 1 h postinfection, these groups received a single intraperitoneal dose of 50 or 100 μg/mouse of ClyJ, ClyJ-3, or Cpl-1 ($n = 12$ for each group), 100 μg/mouse of penicillin G ($n = 12$), or an equal volume of PBS buffer ($n = 12$). To compare the protective efficacies of ClyJ and ClyJ-3 in a low-enzyme dose, female BALB/c mice (6 to 8 weeks old) were injected intraperitoneally with 3.8×10^7 CFU/mouse of *S. pneumoniae* NS26, randomized, and received either a single dose of 40 μg/mouse of ClyJ ($n = 10$), 2 μg/mouse of ClyJ-3 ($n = 10$), or an equal volume of PBS buffer ($n = 10$). The survival rates for all groups were recorded for 10 days.

Data availability. Sequences of ClyJ and its variants ClyJ-1, ClyJ-2, and ClyJ-3 described have been deposited in GenBank under accession numbers MN711694, MN711695, MN711696, and MN711697, respectively.

SUPPLEMENTAL MATERIAL

Supplemental material is available online only.

SUPPLEMENTAL FILE 1, PDF file, 0.7 MB.

ACKNOWLEDGMENTS

This work was supported by grants from the Youth Innovation Promotion Association CAS (to H.Y.), the National Natural Science Foundation of China (no. 31770192 to H.Y. and no. 31570175 to H.W.), the Open Research Fund Program of National Bio-Safety Laboratory, Wuhan (no. 2019SPCAS001 to W.Y.), and the Natural Science Foundation of Henan Province (no. 182300410391 to P.X.).

We are grateful to Jia Wu, Xuefang An, Yun Peng, and Ge Gao from the Core Facility and Technical Support, Wuhan Institute of Virology, for their assistance in animal experiments.

I.E. served as a military service member over the course of this work, which was prepared as part of her official duties. The views expressed in this article are those of the authors and do not necessarily reflect the official policy or position of the Department of the Navy, Department of Defense, or the U.S. Government.

We have no competing financial interests to declare.

REFERENCES

1. Andrade AL, Toscano CM, Minamisava R, Costa PS, Andrade JG. 2011. Pneumococcal disease manifestation in children before and after vaccination: what's new? Vaccine 29(Suppl 3):C2–C14. https://doi.org/10.1016/j.vaccine.2011.06.096.
2. Deng X, Church D, Vanderkooi OG, Low DE, Pillai DR. 2013. *Streptococcus pneumoniae* infection: a Canadian perspective. Expert Rev Anti Infect Ther 11:781–791. https://doi.org/10.1586/14787210.2013.814831.
3. Kim L, McGee L, Tomczyk S, Beall B. 2016. Biological and epidemiological features of antibiotic-resistant *Streptococcus pneumoniae* in pre- and post-conjugate vaccine eras: a united states perspective. Clin Microbiol Rev 29:525–552. https://doi.org/10.1128/CMR.00058-15.
4. Walker CLF, Rudan I, Liu L, Nair H, Theodoratou E, Bhutta ZA, O'Brien KL, Campbell H, Black RE. 2013. Global burden of childhood pneumonia and diarrhoea. Lancet 381:1405–1416. https://doi.org/10.1016/S0140-6736(13)60222-6.
5. Huttner A, Harbarth S, Carlet J, Cosgrove S, Goossens H, Holmes A, Jarlier V, Voss A, Pittet D. 2013. Antimicrobial resistance: a global view from the 2013 World Healthcare-Associated Infections Forum. Antimicrob Resist Infect Control 2:31. https://doi.org/10.1186/2047-2994-2-31.
6. McCarthy M. 2013. CDC calls for urgent action to combat rise of drug resistant pathogens. BMJ 347:f5649. https://doi.org/10.1136/bmj.f5649.
7. Fischetti VA. 2008. Bacteriophage lysins as effective antibacterials. Curr Opin Microbiol 11:393–400. https://doi.org/10.1016/j.mib.2008.09.012.
8. Nelson D, Loomis L, Fischetti VA. 2001. Prevention and elimination of upper respiratory colonization of mice by group A streptococci by using a bacteriophage lytic enzyme. Proc Natl Acad Sci U S A 98:4107–4112. https://doi.org/10.1073/pnas.061038398.
9. Yang H, Zhang Y, Yu J, Huang Y, Zhang XE, Wei H. 2014. Novel chimeric lysin with high-level antimicrobial activity against methicillin-resistant *Staphylococcus aureus* in vitro and in vivo. Antimicrob Agents Chemother 58:536–542. https://doi.org/10.1128/AAC.01793-13.
10. Jado I, Lopez R, Garcia E, Fenoll A, Casal J, Garcia P, Spanish Pneumococcal Infection Study Network. 2003. Phage lytic enzymes as therapy for antibiotic-resistant *Streptococcus pneumoniae* infection in a murine sepsis model. J Antimicrob Chemother 52:967–973. https://doi.org/10.1093/jac/dkg485.
11. Gerstmans H, Criel B, Briers Y. 2018. Synthetic biology of modular endolysins. Biotechnol Adv 36:624–640. https://doi.org/10.1016/j.biotechadv.2017.12.009.
12. Yang H, Yu J, Wei H. 2014. Engineered bacteriophage lysins as novel anti-infectives. Front Microbiol 5:542. https://doi.org/10.3389/fmicb.2014.00542.
13. Loeffler JM, Nelson D, Fischetti VA. 2001. Rapid killing of *Streptococcus pneumoniae* with a bacteriophage cell wall hydrolase. Science 294:2170–2172. https://doi.org/10.1126/science.1066869.
14. Loeffler JM, Djurkovic S, Fischetti VA. 2003. Phage lytic enzyme Cpl-1 as a novel antimicrobial for pneumococcal bacteremia. Infect Immun 71:6199–6204. https://doi.org/10.1128/iai.71.11.6199-6204.2003.
15. Mellroth P, Daniels R, Eberhardt A, Ronnlund D, Blom H, Widengren J, Normark S, Henriques-Normark B. 2012. LytA, major autolysin of *Streptococcus pneumoniae*, requires access to nascent peptidoglycan. J Biol Chem 287:11018–11029. https://doi.org/10.1074/jbc.M111.318584.
16. Lopez R, Garcia E. 2004. Recent trends on the molecular biology of pneumococcal capsules, lytic enzymes, and bacteriophage. FEMS Microbiol Rev 28:553–580. https://doi.org/10.1016/j.femsre.2004.05.002.
17. Bustamante N, Campillo NE, Garcia E, Gallego C, Pera B, Diakun GP, Saiz JL, Garcia P, Diaz JF, Menendez M. 2010. Cpl-7, a lysozyme encoded by a pneumococcal bacteriophage with a novel cell wall-binding motif. J Biol Chem 285:33184–33196. https://doi.org/10.1074/jbc.M110.154559.
18. Varea J, Saiz JL, López-Zumel C, Monterroso B, Medrano FJ, Arrondo JL, Iloro I, Laynez J, Garcia JL, Menéndez M. 2000. Do sequence repeats play an equivalent role in the choline-binding module of pneumococcal LytA amidase? J Biol Chem 275:26842–26855. https://doi.org/10.1074/jbc.M004379200.
19. Buey RM, Monterroso B, Menendez M, Diakun G, Chacon P, Hermoso JA, Diaz JF. 2007. Insights into molecular plasticity of choline binding proteins (pneumococcal surface proteins) by SAXS. J Mol Biol 365:411–424. https://doi.org/10.1016/j.jmb.2006.09.091.
20. Yang H, Gong Y, Zhang H, Etobayeva I, Miernikiewicz P, Luo D, Li X, Zhang X, Dąbrowska K, Nelson DC, He J, Wei H. 2019. ClyJ is a novel pneumococcal chimeric lysin with a cysteine- and histidine-dependent amidohydrolase/peptidase catalytic domain. Antimicrob Agents Chemother 63:e2043-18. https://doi.org/10.1128/AAC.02043-18.
21. Díez-Martínez R, de Paz HD, Bustamante N, García E, Menéndez M, García P. 2013. Improving the lethal effect of Cpl-7, a pneumococcal phage lysozyme with broad bactericidal activity, by inverting the net charge of its cell wall-binding module. Antimicrob Agents Chemother 57:5355–5365. https://doi.org/10.1128/AAC.01372-13.
22. Low LY, Yang C, Perego M, Osterman A, Liddington R. 2011. Role of net charge on catalytic domain and influence of cell wall binding domain on bactericidal activity, specificity, and host range of phage lysins. J Biol Chem 286:34391–34403. https://doi.org/10.1074/jbc.M111.244160.
23. Reinke AA, Gestwicki JE. 2007. Structure-activity relationships of amyloid beta-aggregation inhibitors based on curcumin: influence of linker

length and flexibility. Chem Biol Drug Des 70:206–215. https://doi.org/10.1111/j.1747-0285.2007.00557.x.
24. Collins T, Meuwis MA, Gerday C, Feller G. 2003. Activity, stability and flexibility in glycosidases adapted to extreme thermal environments. J Mol Biol 328:419–428. https://doi.org/10.1016/s0022-2836(03)00287-0.
25. Yang H, Zhang H, Wang J, Yu J, Wei H. 2017. A novel chimeric lysin with robust antibacterial activity against planktonic and biofilm methicillin-resistant *Staphylococcus aureus*. Sci Rep 7:40182. https://doi.org/10.1038/srep40182.
26. Vázquez R, Domenech M, Iglesias-Bexiga M, Menéndez M, García P. 2017. Csl2, a novel chimeric bacteriophage lysin to fight infections caused by *Streptococcus suis*, an emerging zoonotic pathogen. Sci Rep 7:16506. https://doi.org/10.1038/s41598-017-16736-0.
27. Yang H, Linden SB, Wang J, Yu J, Nelson DC, Wei H. 2015. A chimeolysin with extended-spectrum streptococcal host range found by an induced lysis-based rapid screening method. Sci Rep 5:17257. https://doi.org/10.1038/srep17257.
28. Zhao H, Verma D, Li W, Choi Y, Ndong C, Fiering SN, Bailey-Kellogg C, Griswold KE. 2015. Depletion of T cell epitopes in lysostaphin mitigates anti-drug antibody response and enhances antibacterial efficacy in vivo. Chem Biol 22:629–639. https://doi.org/10.1016/j.chembiol.2015.04.017.
29. Blazanovic K, Zhao H, Choi Y, Li W, Salvat RS, Osipovitch DC, Fields J, Moise L, Berwin BL, Fiering SN, Bailey-Kellogg C, Griswold KE. 2015. Structure-based redesign of lysostaphin yields potent antistaphylococcal enzymes that evade immune cell surveillance. Mol Ther Methods Clin Dev 2:15021. https://doi.org/10.1038/mtm.2015.21.
30. Resch G, Moreillon P, Fischetti VA. 2011. A stable phage lysin (Cpl-1) dimer with increased antipneumococcal activity and decreased plasma clearance. Int J Antimicrob Agents 38:516–521. https://doi.org/10.1016/j.ijantimicag.2011.08.009.
31. Seijsing J, Sobieraj AM, Keller N, Shen Y, Zinkernagel AS, Loessner MJ, Schmelcher M. 2018. Improved biodistribution and extended serum half-life of a bacteriophage endolysin by albumin binding domain fusion. Front Microbiol 9:2927. https://doi.org/10.3389/fmicb.2018.02927.
32. Hermoso JA, Monterroso B, Albert A, Galán B, Ahrazem O, García P, Martínez-Ripoll M, García JL, Menéndez M. 2003. Structural basis for selective recognition of pneumococcal cell wall by modular endolysin from phage Cp-1. Structure 11:1239–1249. https://doi.org/10.1016/j.str.2003.09.005.
33. Ho SN, Hunt HD, Horton RM, Pullen JK, Pease LR. 1989. Site-directed mutagenesis by overlap extension using the polymerase chain reaction. Gene 77:51–59. https://doi.org/10.1016/0378-1119(89)90358-2.
34. Etobayeva I, Linden S, Alem F, Harb L, Rizkalla L, Mosier P, Johnson A, Temple L, Hakami R, Nelson D. 2018. Discovery and biochemical characterization of PlyP56, PlyN74, and PlyTB40—Bacillus specific endolysins. Viruses 10:276. https://doi.org/10.3390/v10050276.
35. Yang J, Yan R, Roy A, Xu D, Poisson J, Zhang Y. 2015. The I-TASSER Suite: protein structure and function prediction. Nat Methods 12:7–8. https://doi.org/10.1038/nmeth.3213.